A&A manuscript no.
(will be inserted by hand later)

Your thesaurus codes are:
13(19.07.1;14.03.1; 16.08.1)

ASTRONOMY
AND
ASTROPHYSICS
10.8.1995

The Tycho Star Mapper Background analysis *

A. Wicenec and F.van Leeuwen

[1] Institut für Astronomie und Astrophysik (Astronomie) der Universität Tübingen, Waldhäuserstr. 64, D–72076 Tübingen, FRG
[2] Royal Greenwich Observatory, Madingley Road, Cambridge CB3 0EZ, UK

Received date; accepted date

Key words: numerical methods - instruments - magnetosphere - Hipparcos

Abstract. The Hipparcos star mapper detector background signal has been analyzed in the Tycho reductions for contributions due to the diffuse galactic light. The methods are presented by which the contributions from the two fields of view of the telescope are separated after elimination of background variations due to the radiation environment (Van Allen belts). A complete sky background map, with a resolution of 0.25 square degrees and based on the data accumulated through almost two years of the mission is presented.

1. Introduction

The Hipparcos satellite has scanned the sky closely following a pre-defined scanning law (Perryman and Vaghi, 1989). This scanning law provided a complete coverage of the sky every 6 months, while keeping the two fields of view of the telescope at least 47 degrees away from the direction to the sun. This was obtained by letting the satellite rotate around its z-axis once every 2^h8^m, and letting the satellite's z axis rotate at a constant angle of 43 degrees around the sun direction, following the sun in its apparent motion along the ecliptic and performing 6.4 revolutions per year.

Due to the failure of the apogee boost motor, the satellite remained for the entire mission in a highly eccentric orbit, with perigee at 400 to 600 km from the earth surface, and apogee near geostationary level. The orbital period, close to 10^h40^m, was chosen such that it was very close to 5 complete revolutions of the satellite. As a result, features on the sky encountered during the rotation of the satellite tend to repeat at nearly the same orbital phase from one orbit to the next. The orbital phases of occultation gaps and crossings of the galactic and the ecliptic planes drift slowly from one orbit to the next. This can be seen in Fig. 5.

The detectors in the focal plane of the telescope looked at the sky at any one time in two directions, separated by what is generally referred to as the basic angle (58 degrees). Thus, when measurements of the background were made, these measurements contained contributions from two different parts of the sky, without direct means of separation. In addition, the detectors showed sensitivity to the very high energy particles in the electron and proton radiation belts (see Daly et al., 1994). The radiation environment for the satellite is varying all the time both as a result of the orbit and as a result of changes in the activity levels of the radiation belts. This was in particular the case soon after bursts of solar activity.

Table 1. Contributions to the Star Mapper background

Contributor	cycle	maximum
Galactic	2^h08^m	3
Zodiacal	2^h08^m	2.4
Stray light	10^h40^m	15.
Radiation	10^h40^m	saturation

At some occasions, near to Earth and Moon occultations, there was sometimes also a contribution from stray light, especially towards the second half of the mission, when shutter closing times had been brought down to a minimum. Table 1 summarizes the various effects and their maximum contribution as they were observed. The present paper will concentrate mainly on elimination of the radiation belt contributions, and the accumulation of the diffuse galactic background. A study separating the zodiacal light from the galactic background is still going on. First we present a overview of the relevant steps in

Send offprint requests to: A. Wicenec

*Based on observations made with the ESA Hipparcos satellite the data reductions. This is followed by a description of the separation process. Section three describes the accumulation of results, and the last section presents a short discussion of the results.

2. Overview of the data and first reductions

The star mapper detectors on board the Hipparcos satellite were equipped with a prism, splitting the light into a blue (B_T) and a visual (V_T) channel. The light across the entire star mapper grid was recorded by photomultipliers, one for the B_T and one for the V_T channel. Sampling took place at 600 Hz. The data were collected in telemetry formats lasting 10.667 seconds, giving 6400 samplings per format. The star mapper detectors have been used in two different ways. By the satellite and the Hipparcos data analysis they were used to establish or reconstruct the pointings of the three satellite axes. For this purpose mainly stars from the Hipparcos Input Catalogue (Turon et al., 1989) were used. In the Tycho experiment, the star mapper data was the main data stream, which was used to perform a complete astrometric and photometric survey of the sky down to its limiting magnitude (Høg et al., 1989).

The methods used for determining the background in the star mapper signal over the time spanned by one format, 10.6667 seconds, is described in detail in Wicenec and Bässgen (1992) and Wicenec (1995). The method used in the Hipparcos reductions is described in Canuto et al. (1989). In the calibration of the flux the photometric calibration (see Scales et al. 1992) of the main data reduction chain for that time interval was used. A total of 37 months of data has been collected, with an average efficiency of 60 percent (eliminating the worst contributions of the radiation environment), thus giving a total of approximately 5 million background estimates derived from data of one format each. After separation between the two fields of view, this could provide around 60 measurements per 0.25 square degree on the sky. The quality of 50 percent of these make them unsuitable for mapping.

The coordinates of every background measurement are evaluated from the known parameters of the nominal scanning law of the satellite which is followed to within $10'$, sufficiently accurate for the present investigation, considering the fact that over a timespan of one format the detectors cover an area of $30'$ by $40'$. In the Hipparcos data reduction the background is based on a much shorter time span, $5/12s$, equivalent to $1.1'$ by $40'$. But there data are accumulated and averaged over time spans of 38 seconds, giving an average background in an area of $105'$ by $40'$. Coordinates were calculated in the galactic reference frame and in the heliotropic ecliptic reference frame. In the heliotropic reference frame, the ecliptic latitude, and longitude with respect to the longitude of the sun, were derived for the zodiacal light accumulation.

3. Separation procedures

All Tycho measurements have some intrinsic symmetries due to the orbital period, the rotation period and the fields of view. These symmetries are more or less obvious in the data. The orbital period is visible due to the periodic crossing of the satellite of the van Allen belts which causes a periodic raise of the background. However the structure and the amplitude of these disturbances is rather undefined and thus the global structure of the background is not reproduced after one orbital period (3600 formats) . The rotation period is visible in the fine structure of the background, because the motion of the z-Axes of the satellite (perpendicular to the plane defined by the directions of the fields of view) is only $0\overset{\circ}{.}41$ during one rotation. That means that due to the length of the slit system of $0\overset{\circ}{.}667$ ($40'$) the same region of the sky is visible within more than one rotation of the satellite. The net effect is that the background value of a given format is almost reproduced after one rotation period (720 formats) if small scale variations of the background are neglected.

3.1. The orbit dependent components

The separation of the orbit dependent components uses the knowledge about the periodicity of the background for consecutive rotations. Starting with raw background data of approximately one day , a so–called 'reference circle' (RC) is evaluated.

The RC contains the background data during one rotation of the satellite, and thus has a length of 720 formats. It holds the lowest measured background values for every of the 720 formats of all rotations of the satellite within the selected day, and should be relatively free of contributions from the radiation environment. Fig. 1 shows the division of slightly more than one day of background data into rotation circles (rotations) of the satellite starting at an arbitrary point. Fig. 2 shows the RC (full line) for the data used in Fig. 1. A sufficiently long period free from disturbances by the radiation environment is not always available. To deal with data when an RC can not be obtained the RC of the preceding day is used as starting point in the analysis of the new data. Thus the evaluation of the RC is like an iteration, and to start this iteration a period with very good data is selected, i.e. a period where the disturbances due to the orbit are very low. Since the number of large data gaps during the mission is rather low, it is possible to treat most of the mission with only a few starting points.

To correct all other data obtained, the RC is smoothed by a modified Akima interpolation/ approximation (Akima, 1970), which uses a linearly declining law to model the smoothing influence of an interval of 25 points around every of the 720 points of the RC. The result is a strongly smoothed RC, where most of the small scale variations are removed. All the data is subsequently collected

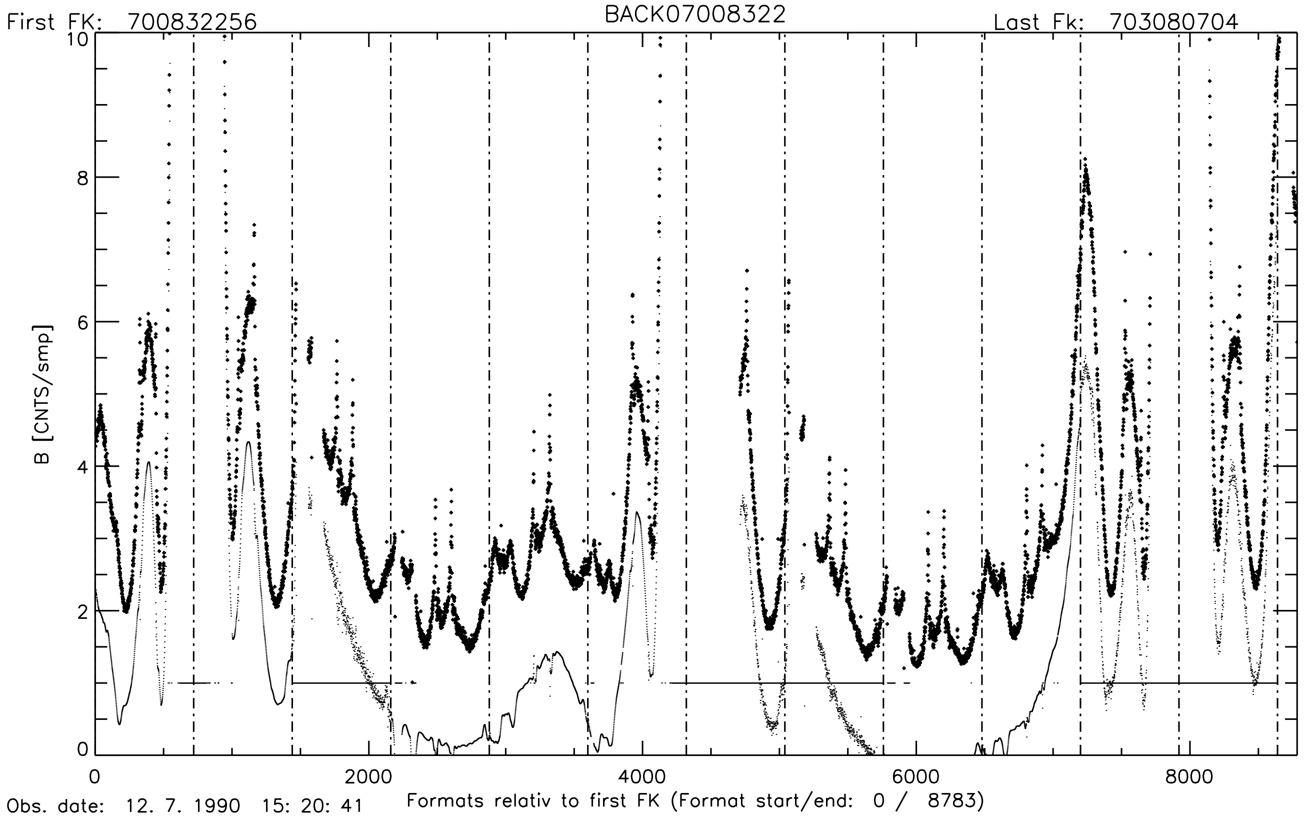

Fig. 1. This figure shows some of the first steps of the data reduction. The small crosses mark the original B-channel background data obtained during 8783 telemetry formats (lower x-axes) i.e. slighly more than one day. The dotted curve mark all the individual correction values applied to the original values to correct for the van Allen Belt influences. The dotted horizontal line(s) at 1 count/sample mark the regions where the background is not used for further reductions due to some quality flagging. The division of the corrected background data into arbitrary rotations of the satellite is indicated by the vertical lines in this figure.

in groups of 720 formats and smoothed by the same method. The differences between the smoothed data and the smoothed RC are attributed to the orbital component in the background (the radiation environment). These differences are then used to correct the original, not smoothed data, to obtain the local small scale variations which form the input data for our further investigation.

Fig. 2 shows the power and the limitations of this procedure, where the upper curve (marked by small squares) represents the original data, the lower curves of small crosses the corrected data and the full line marks the RC (not smoothed). For the first part up to format 550 the result of the correction is very satisfying, but after this point the corrected data show a clearly improbable behaviour. This is due to the very steep gradient of the background in the original data (the value at format 600 is already more than 400 counts per sampling period (600 Hz)). Above format 612 the rotation circle is exactly the same as the RC, because the correction algorithm has rejected some of the original data points. The small scale variations of the rotation circle are almost completely preserved. Most of the suspect points in this corrected rotation circle will not be used for the mapping, because they are weighted down to almost zero, due to the high correction level at this point.

During the development of the method described above it turned out, that the correction of the orbital components is by far the most complicated process within the reduction of the background data. Because of the high variability of the structure and amplitude of the radiation related component, it was not possible to establish a model covering all the data and it was thus necessary to correct every orbit individually.

3.2. The separation of the fields of view

Compared with the problems due to the orbital motion of the satellite, the separation of the fields of view is rather straightforward. This process also uses the knowledge of internal symmetries of the data and some assumptions on the scale of the fine structure of the sky background.

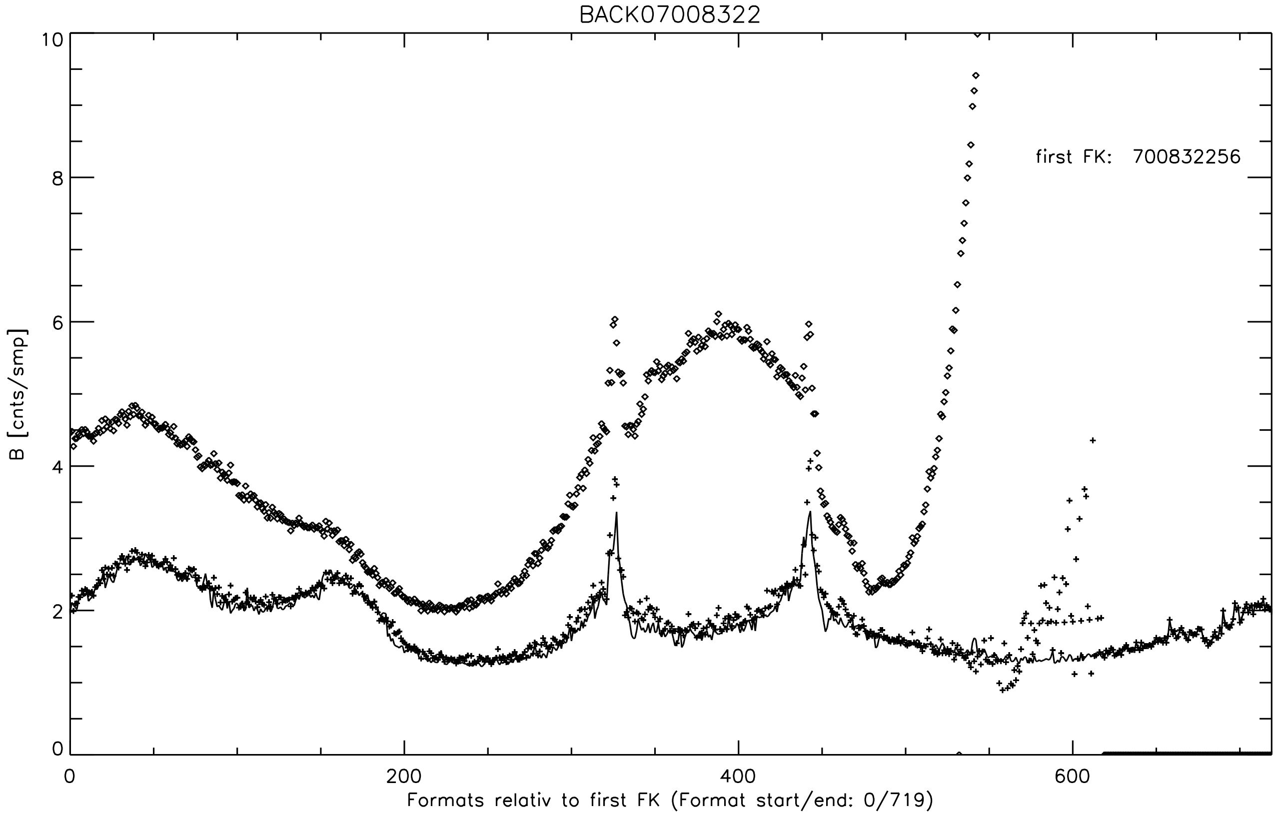

Fig. 2. Correction of the orbital component within one rotation of the satellite (the first rotation in Fig. 1). Upper curve (small squares) is the original data, the small crosses mark the corrected rotation circle and the full line marks the RC. More details are explained in the text.

1. All real features of the sky background have to appear twice in one rotation circle, i.e. from either of the fields of view.
2. The spin phase of the satellite is part of the nominal attitude and is kept to within $10'$ of its nominal value at any time: the satellite rotates at an average angular velocity of $168''\!.75s^-1$, equivalent to $0^\circ\!.5$ per format. Thus, given the basic angle of 58°, a feature appearing in the preceding (leading) field of view (PFOV) in format x should appear in the following (trailing) field of view (FFOV) in format $x+116$.
3. The background for a given region in one field of view should be the same when viewed through the other field of view, up to a constant difference in the response between the fields.
4. There are no background structures below an area of $10' \times 10'$. This assumption is in principle equivalent to the one above.

The high asymmetry of the basic angle of the telescope (58°) to one full circle (360°) may be expressed by the smallest multiple, (k) of both angles.

$$k = 10\,440 \tag{1}$$

assuming that the motion of the z-axes is switched off this value of k means that both fields of view would observe exactly the same regions of the sky, only after the time span ΔT of

$$\Delta T \cong 10440 \times \frac{32}{3} = 1856 \quad min = 30.9334 \quad h \tag{2}$$

That means in turn after $N_i = 180$ steps of 58°. Together with the assumptions made above this means, that it is possible to separate the differences of the background measured in format x and format $x+116$ by an 180 step iteration. These differences can be assigned definitely to one of the fields of view. A complete separation of the fields of view is however only reached, if the differences could be calibrated to absolute values. The physical meaning of such a calibration are the components of the background which are common for both fields of view, such as the rest of the particle background, the minimum of the sky background (as a superposition of all components of the background) and the instrument dark and stray–light count–rates. The calibration is carried out by adding a constant term (K_e) equivalent for both fields. The complete separation may be written by the following formulae, where

$PFOV_t$ and $FFOV_t$ are the differences derived by a function SEP_FOV, which carries out the iteration and RC is the rotation circle under view.

$$(PFOV_t, FFOV_t) = SEP\_FOV(RC) \tag{3}$$

together with

$$K_e = \frac{1}{2}(Median(RC - (PFOV_t + FFOV_t))) \tag{4}$$

yields

$$PFOV_e = PFOV_t + K_e \tag{5}$$

$$FFOV_e = FFOV_t + K_e \tag{6}$$

where $PFOV_e$ and $FFOV_e$ are the calibrated rotation circles for the preceding and following field of view, respectively.

In practice the function SEP_FOV is not just an iteration, because there are some difficulties with the use of real data, originating in local violations of assumption 4. Such violations are due to very dense sky regions or single very bright stars. The effect of such violations is additive and the iteration spreads such a violation over the whole circle, yielding nonsense results. The tests carried out during the development of the methods showed, that the iteration conjugates after as little as 6 steps to an intermediate solution. However this solution is disturbed by waves with a period of 116 formats if the starting point is not carefully chosen. An automatic procedure to choose this starting point is not applicable, due to the complicated structure of the superposition of the different background components. It turns out, that it is possible to correct most of these waves by just shifting the solution of the FFOV to the solution of the PFOV, summation and division by two. This is due to the fact that the solutions for the fields are independent in view of the iteration, but they should be physically the same when one of the resulting circles is shifted by 116 formats. The rest of the waves are suppressed by using a FFT algorithm.

The function SEP_FOV is defined by the following equivalent formulae for the fields of view:

$$PFOV_t(s..s+115) = RC(s..s+115) - \sum_{i=1}^{6}(-1)^i \times RC(j..j+115) \tag{7}$$

$$FFOV_t(s..s+115) = RC(s..s+115) - \sum_{i=1}^{6}(-1)^i \times RC(j..j+115) \tag{8}$$

with the starting value s

$$s \in \{0, 116, 232, 348, 464, 580, 696\} \tag{9}$$

and

$$j = \begin{cases} (720 + s - 116i) \quad mod \quad 720 & for \quad PFOV \\ (s + 116) \quad mod \quad 720 & for \quad FFOV \end{cases} \tag{10}$$

Since for real data it is not possible to determine the error of this procedure some sets of test data have been produced. The method to produce test data is just to produce a PFOV circle, shift it by 116 formats to get a FFOV circle and add them to arrive at a rotation circle. Such test circles have been used to determine the error of the separation. The relative error was in every case below $\pm 10\%$ and the mean absolute error was below 2%.

3.3. The zodiacal light component

The zodiacal light (ZL) component causes the highest raise of background next to the orbital component. Although it is a real sky background feature it is rather hardly disturbing investigations of the other more distant sources of sky background. Since the ZL apparently varies with the motion of the satellite around the sun, the structure appears very nonuniform in the mapping (cf. Fig. 6). The separation of the ZL component is possible by using the knowledge of this variation and some external calibration. However this procedure needs the data to be converted into the ecliptic coordinate system and re–reduced. This has not been carried out with the incomplete data set and thus the ZL component is only dimmed down by the weighted median used to calculate the background value for each of the mapping pixels. The structure due to the superposition of the scanning of the sky and the variation of the ZL is clearly visible in Fig. 6.

4. Results

The mapping procedure is a straightforward (whilst lengthy) process, which should not be described here in detail. The result for the time interval given above and the B-channel is given as a color coded Aitoff projection map in Fig. 6, where the range is 25 up to 350 $S_{10}(B)_{AOV}$. The galactic coordinates (l^{II}, b^{II}) are reproduced with the galactic center in the center of the map and the longitude running to the left.

4.1. Quantitative comparison

In order to get a feeling of the quality of the results we have chosen the measurements of the Pioneer 10 satellite reduced and described in detail by Toller (1981), and the results presented by C. Classen (1979) in her thesis. The latter one is not shown here, but the results do not differ very much from those of Toller. Fig. 3 shows the background in the galactic plane ($b^{II} = 0$ deg) for both the Pioneer (stars) and the Tycho (crosses) measurements. Since the resolution of the published Pioneer measurements is around 4 sq. deg. the given values have been interpolated

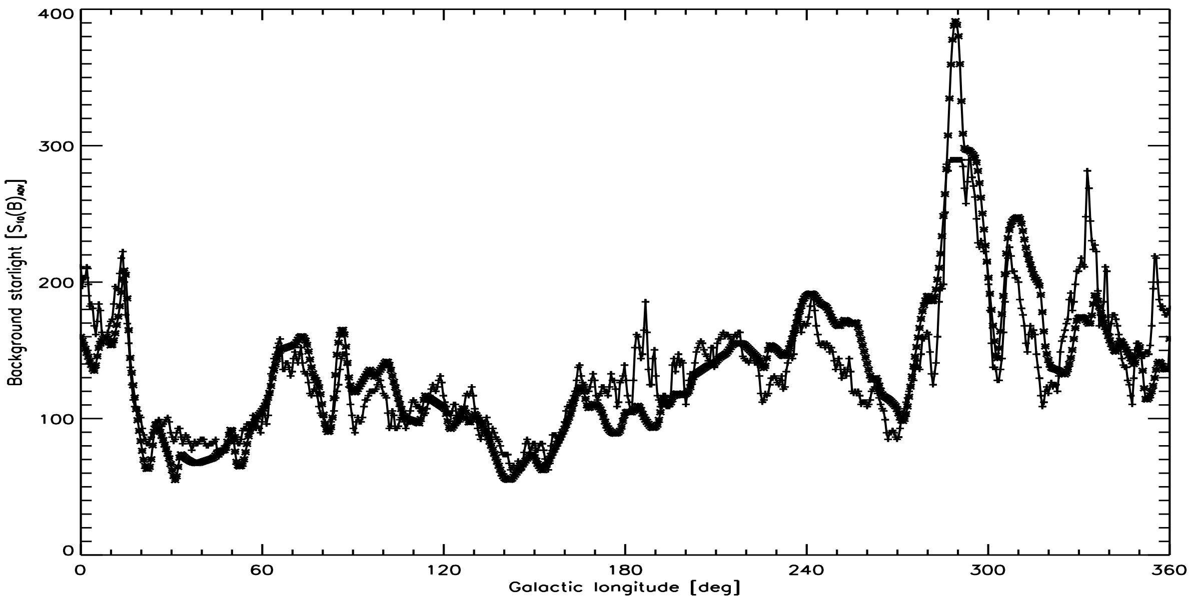

Fig. 3. The background in the galactic plane ($b^{II} = 0$) as measured by the Pioneer satellite (*, interpolated) and by Hipparcos/Tycho (+).

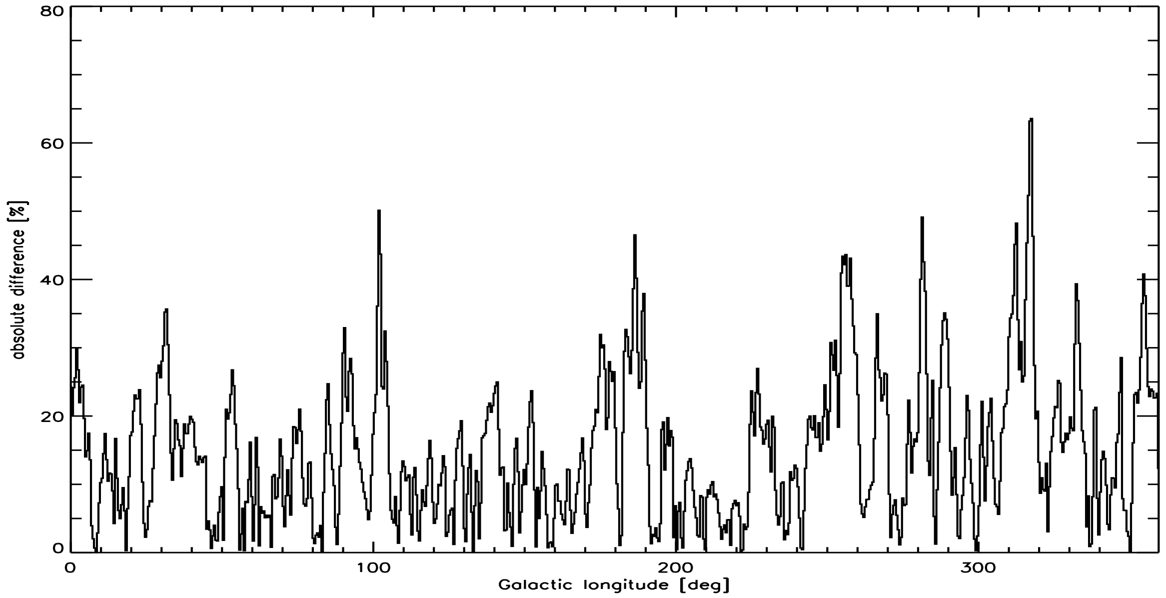

Fig. 4. The absolute difference in percent of the curves given in Fig. 3. The mean difference is only 1.3 %, the mean absolute difference is 12.8 %, i.e. most of the differences are caused by the lower resolution of the Pioneer data.

to the same resolution as the Tycho measurements. This interpolated array has been used to produce Fig. 4, which shows the absolute difference in percent of the curves in Fig. 3. The mean difference is only 1.3 %, the mean absolute difference is 12.8 %, i.e. the global background value is the same for this subset of data and most of the individual values in the galactic plane have a difference of less than 20 %. Most of the individual peaks of Fig. 4 are rather narrow, indicating that the missing fine structure of the Pioneer data is responsible for these differences. Broader peaks appear around 35, 100, 180, 250, 315, 330 and 360/0 degrees. The peaks around 360/0, 180, 35 and 330 degrees, where the Tycho background appears to be higher are due to the incomplete subtraction of the zodiacal light (cf. section 'Outlook').

For a two-dimensional comparison Fig. 7 is given, which contains the region of the southern coal sack. This region has been investigated in detail by different authors, e.g. Seidensticker et al. (1982) and Mattila (1973). The direct comparison of Fig. 7 with the figures given in these papers reveals an excellent correspondence of the structure of the maps. The values for the isophotes given by Seidensticker et al. (1982) are higher by a factor of 1.2. The comparison with the results of Toller (and references therein) reveals that these values are also lower than those values given by Seidensticker. The factors vary between 1.1 and 1.25.

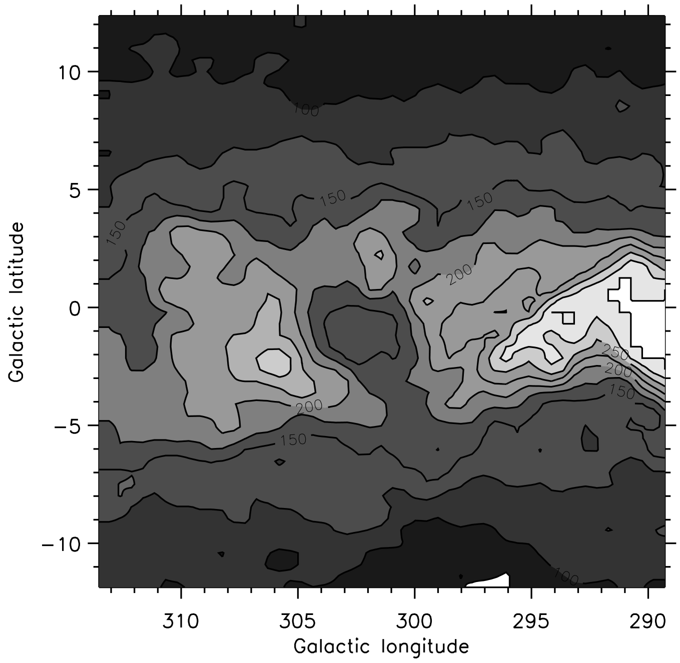

Fig. 7. Isophotal map of the southern coal sack region. Isophotes run from 50 to 300 S_{10} units in steps of 25 units. Isophotes are smoothed to enhance their visibility.

5. Conclusion and Outlook

A reduction of the B-channel background data of almost 620 days of the nominal Hipparcos/ Tycho mission has been carried out. The resulting map of the B- background verifies the methods developed to separate the orbital components and the superposed fields of view of the Hipparcos satellite. The resolution of the map of 0.25 sq. deg. is unprecedented for an all-sky map and the quality of the data is at least as good as previous measurements for limited sky regions. The number of individual background measurements of ≈ 10 million per channel sets up a unique database, with a wide range of possible investigations. Since the raw data is separated (not corrected) in the different components, the data for these components is also available. That means that the particle component is available as well as the zodiacal light. Thus the influence of solar activities to the direct satellite environment, the drift rate of particles in the outer magnetosphere or the shape of the magnetosphere could be investigated.

The zodiacal light is scanned over the whole sphere with the exception of two cones with cone angles of 47 deg. around the directions to the sun and the Gegenschein, respectively. Also with respect to the zodiacal light this database is unprecedented in size for a space experiment. The zodiacal light component will be separated by using the knowledge of the variations caused by the satellite movement and a model of the zodiacal light.

After subtraction of the zodiacal light component the integrated starlight, the diffuse galactic light and the extragalactic light are the sources of the rest of the background light. Each of these components are of their own special interest, however the disentangling of them is rather difficult and only possible under some restrictive assumptions. Nevertheless the Tycho background database gives access to new high resolution background data for each of the different topics.

Acknowledgments: This work was supported by the Bundesministerium für Forschung und Technologie under grants No. 010085029. We would like to thank G.N. Toller for sending his thesis, D. Mink for his maps of the Guide Star Catalogue and the referee Prof. J. Pfleiderer for his remarks and suggestions.

References

Bässgen G., Wicenec A., Andreasen G.K., Høg E., Wagner K., Wesselius P.R., 1992, A&A 258(186)

Classen C., Doctoral thesis, University of Bonn, 1976

Daly E.J., van Leeuwen F., Evans H.D.R, Perryman M.A.C., 1994, IEEE Trans.Nucl.Sci. (in press)

Høg E., Bastian U., Egret D., Grewing M., Halbwachs J.L., Wicenec A., Bässgen G., Bernacca P.L., Donati F., Kovalevsky J., van Leeuwen F., Lindegren L., Pedersen H., Perryman M.A.C., Petersen C., Scales D., Snijders M.A.J., Wesselius P.R., 1992, A&A 258(177)

Mattila K., Sterne und Weltraum, 1973, 12(246)

Perryman M.A.C., Vaghi S., 1989, in ESA SP-1111, I(11)

Perryman M.A.C. ed., 1989, The Hipparcos mission, ESA SP-1111, Vol. I-III

Scales D., Snijders M.A.J., Andreasen G.K., Grenon M., Grewing M., Høg E., van Leeuwen F., Lindegren L., Mauder H., 1992, A&AS 258(211)

Seidensticker K.J., Schmidt-Kaler T., Schlosser W., 1982, A&AS 114(60)

Toller G.N., Doctoral thesis, State University N.Y., Stony Brook, 1981

Wicenec A., Bässgen G., Tycho background determination and monitoring, 1992, A&AS 258(206)

Wicenec A., Doctoral thesis , University of Tübingen, 1995

This article was processed by the author using Springer-Verlag LaTeX A&A style file *L-AA* version 3.

Fig. 5. The accumulated background data for 800 orbits at the start of the mission. Every vertical line represents one orbit. The color scale represents the $log(Back_B)$, with blue for the lowest levels and white for the highest. Black areas represent times when no data was collected due to occultations and ground-station non-availability.

Fig. 6. The B-background of the sky as seen from the Tycho experiment on–board the Hipparcos satellite. Color coding is in $S_{10}(B)_{AOV}$ units in the range of 25 to 350. The zodiacal light has not been subtracted and produces the nonuniform structure following the ecliptic. The map is an Aitoff projected galactic coordinates with the longitude running from the center of the map to the left. The color scale runs from blue for the lowest levels via green, yellow and red up to black for the highest levels.